ELSEVIER

Contents lists available atScienceDirect

Materials Letters

journal homepage:www.elsevier.com/locate/mlble



Synthesis of nanoporous calcium carbonate spheres using double hydrophilic block copolymer poly(acrylic acid-b-N-isopropylacrylamide)



Sudhina Guragain ^a, Nagy L. Torad ^{a,b}, Yousef Gamaan Alghamdi ^c, Abdulmohsen Ali Alshehri ^c, Jeonghun Kim ^d, Bishnu Prasad Bastakoti ^{a,f}, Yusuke Yamauchi ^{a,b,d,e,f}

- ^a International Center for Materials Nanoarchitectonics (WPI-MANA), National Institute for Materials Science (NIMS), 1-1 Namiki, Tsukuba, Ibaraki 305-0044, Japan ^b College of Chemistry and Molecular Engineering, Qingdao University of Science and Technology, Qingdao 266042, China ^c Department of Chemistry, King Abdulaziz University, P.O. Box. 80203, Jeddah 21589, Saudi Arabia
- d School of Chemical Engineering and Australian Institute for Bioengineering and Nanotechnology (AIBN), The University of Queensland, Brisbane, QLD 4072, Australia Department of Plant and Environmental New Resources, Kyung Hee University, 1732 Deogyeong-daero, Giheung-gu, Yongin-si, Gyeonggi-do 446-701, South Korea

article info

Article history: Received 13 June 2018 Received in revised form 9 July 2018 Accepted 14 July 2018 Available online 17 July 2018

Keywords:
Nanoporous materials
Micelles
Calcium carbonate
Double hydrophilic block copolymer
Drug release

abstract

We report self-assembly of double hydrophilic block copolymer poly(acrylic acid-b-Nisopropylacrylamide) in aqueous solution. Self-assembly of calcium ions chelated complex micelles upon mineralization reaction forms calcium carbonate ($CaCO_3$) sphere. High porosity on $CaCO_3$ spheres can accommodate a large amount of anticancer drug (doxorubicin) and achieve sustainable drug release.

2018 Elsevier B.V. All rights reserved.

1. Introduction

Calcium carbonate (CaCO₃) is a natural mineral with excellent biocompatible and biodegradable properties. Over the recent decades, CaCO₃ based nano/micro particles have been utilized as biomaterials for tissue engineering [1] and several industrial applications such as fillers in paper, plastic and rubber [2]. The porous CaCO₃ is a suitable novel carrier for anticancer drug and bioactive proteins [3]. Due to pH sensitive dissolution of CaCO₃, its structure is well maintained in neutral environment, while slightly acidic environment triggers the release of payloads. Gong et al. reported self-assembled polymer/CaCO₃ hybrid nano-vesicles for multiple drug delivery that showed enhanced uptake, stability and pH sensitive delivery [4]. Superparamagnetic CaCO₃ mesocrystals served as drug and gene co-delivery vehicle for different stages of cancer therapy. Doxorubicin, Au-DNA and Fe₃O₄@silica nanoparticles loaded mesocrystalline CaCO₃ particles were designed to shield functional sections from degradation and phagocytosis

↑ Corresponding authors at: International Center for Materials Nanoarchitectonics (WPI-MANA), National Institute for Materials Science (NIMS), 1-1 Namiki, Tsukuba, Ibaraki 305-0044, Japan (Y. Yamauchi and B.P. Bastakoti).

E-mail addresses: bishnubastakoti@hotmail.com (B.P. Bastakoti), Yamauchi. Yusuke@nims.go.jp (Y. Yamauchi).

https://doi.org/10.1016/j.matlet.2018.07.060

0167-577X/2018 Elsevier B.V. All rights reserved.

during circulation. The system displayed high competence of intracellular delivery [5].

Several approaches have been used for the preparation of CaCO₃ nano/micro particles. Zhao et al. reported template-free synthesis of hollow CaCO₃ spheres by an aggregation mechanism [6]. Polysaccharides, proteroglycans [7], double hydrophilic block copolymer (DHBC)-surfactant mixtures [8], fatty acid Langmuir monolayers [9], liquid crystals [10] have been used for controlling CaCO₃ crystal growth. Compared to the template-free synthesis, template method allows easy control over the size and composition and supple modification of physical and chemical properties of the resulting particles. There has been growing use of the polymeric micelles of amphiphilic block copolymers as a template to fabricate porous inorganic particles [11,12].

In this study, we report an environmental friendly method to synthesize nanoporous CaCO3 spheres by employing DHBC of poly(acrylic acid-b-Nisopropylacrylamide) (PAA-b-PNIPAM) as a template. The polymer is molecularly dissolved in water at room temperature, while at temperature higher than the lower critical solution temperature (LCST) of PNIPAM, PNIPAMcore/PAAcorona micelles are formed. Here, after incorporation of Ca²⁺ ions into the anionic PAA, Ca2+/PAA-core/PNIPAM-corona micelles were obtained at room temperature. Addition of carbonate ions resulted into the formation of CaCO₃/polymer hybrid particles. All the synthesis was carried out in water and

S. Guragain et al. /Materials Letters 230 (2018) 143-147 the removal of the sacrificial template was carried out by simply dispersing the spheres in water, without the need of calcination or hazardous organic solvents.

2. Experimental section

Synthesis of porous CaCO3 spheres. 1.5 g of CaCl2 was added to 5 mL of 0.1 g L1 of aqueous solution of PAA-b-PNIPAM. The solution was stirred at room temperature (ffi25 C) for 1 h. 1.08 g of (NH₄)₂CO₃ was then added to it and the solution was stirred at room temperature (ffi25 C) for next 3 h. The solution was then centrifuged and washed with water several times. The sample was then dried in an oven at 50 C for 24 h.

3. Results and discussion

PAA-b-PNIPAM is a DHBC and exists as unimers in aqueous solution below the LCST of PNIPAM in basic pH [13]. The molecular structure is shown in Fig. 1. The presence of strongly interactive carboxyl functionalized PAA-block and temperature sensitive PNIPAM-block makes the polymer a switchable amphiphiles [13]. The complexation of anionic electrolytes with divalent metal ions has been widely investigated [14,15]. Under basic conditions, PAA block binds with metal ions forming insoluble complex that eventually leads to the formation of micelles of Ca²⁺/PAA-bPNIPAM at room temperature. The size of the Ca²⁺/PAA-core/ PNIPAM-corona micelles was 120 nm, as obtained by the DLS measurement at 25 C. When the temperature increased to above 33 C, the PNIPAM-core/PAA-corona micelles were formed, and the hydrodynamic diameter remained constant (150 \pm 5 nm) till 50 C.

We carried out the mineralization of CaCO₃ on Ca²⁺/PAA-bPNIPAM aggregates. The formation mechanism of CaCO₃ spheres is shown in Fig. 1. The addition of Ca2+ ions into polymer solution formed a Ca2+/PAA-b-PNIPAM complex. Carbonate ions reacted with the Ca2+ ions to start mineralization of CaCO₃. The particles are spherical and uniform with an average size of about 1.5 mm (Fig. 2a). SEM (Fig. 2a-b) and TEM (Fig. 2c-d) images of single sphere after the removal of polymer shows the presence of thorough porosity. We also investigated the LCST behavior of block copolymer in mineralization reaction. The size of the spheres prepared at 45 C is larger than that prepared at 25 C (Fig. 2e). At 45 C, i.e. above the LCST of PNIPAM, the polymer in solution exists as micelles (PNIPAM-core/PAA-corona) even before complexation with Ca²⁺ions. The addition of Ca²⁺ ions results in less stable colloidal dispersion to prepare larger-sized spheres with less porosity. SEM image of CaCO3 particles in the absence of polymer template shows cubical shaped particles with size 4 mm (Fig. 2f).

The crystalline properties of the obtained spheres were confirmed by an XRD analysis. The resultant XRD pattern is presented in Figure S1. The co-existence of calcite and vaterite phases of CaCO₃ in the spheres is confirmed. All the peaks can be assigned to be calcite phase (JCPDS 01-083-0578) and vaterite phase (JCPDS 00-033-0268). The peak with maximum intensity at 2h = 29.48 corresponds to the reflection from (1 0 4) plane of calcite phase (JCPDS 01-083-0578). N₂ adsorption-desorption isotherm was measured to investigate the porosity and the surface area of CaCO3 spheres. Figure S2 shows the N2 adsorption-desorption isotherm with a small hysteresis loop. The BET surface

area is around 82 m2 g1.

CaCO3 is remarkably suitable drug carrier among many inorganic materials because of its excellent biocompatibility and biodegradability. Hence, we employed our spheres for loading DOX. The drug loading capacity of CaCO3 spheres was 197 mg of DOX per gram of CaCO3. The release percentage was calculated according to the following equation.

The release of DOX from spheres was measured spectrophotometrically. Figure S3 shows the release profile of drug molecules. Here, A_t and A₁ represents the absorbance of bulk aqueous phase at time t and 1, respectively. A progressive and sustained release is observed over a prolonged period. Here the release kinetic process was studied using first order, Higuchi, Hixson-Crowell and Korsmeyer-Peppas models [16].

Firstorder :
$$\log 100 \delta$$
 WP $\frac{1}{2} \log 100 \text{ K}_1 \text{t}$

Higuchi :W ¼
$$K_H t^{1=2}$$

Hixson - Crowell :
$$\tilde{0}100 \text{ Wp}^{1=3} \% 100^{1=3} \text{ K}_{HC}t$$

Korsmeyer Peppas :
$$\underline{}^{t}$$
 \times Kt^{n} δ^{5}

where K₁, K_H, K_{HC} and K are drug release constants of the aforementioned first order, Higuchi, Hixson-Crowell and Korsmeyer-Peppas models reflecting the design variables in the system (i.e., the diffusivity of a drug in solvent and the structural properties of hosts), W is the proportion of drug release at time t, M_t/M₁ is the fractional release of drug into the dissolution media, Mt is the release accumulation, M is the total release amount, and n is the release exponent

indicative of the drug release mechanism.

1

To study the release mechanism of DOX, the release kinetics was further examined, and the experimental data were fitted with different release kinetic models (Eqs. (2)-(5)). Clearly, good linear plots are obtained for DOX released from CaCO3 spheres and the release kinetic parameters are determined from Fig. 3. The K₁, K_H and K_{HC} values are determined from the gradient of the kinetic

Fig. 1. Schematic representation of formation of nanoporous $CaCO_3$ spheres with PAA-b-PNIPAM block copolymer. S. Guragain et al. / Materials Letters 230 (2018) 143–147

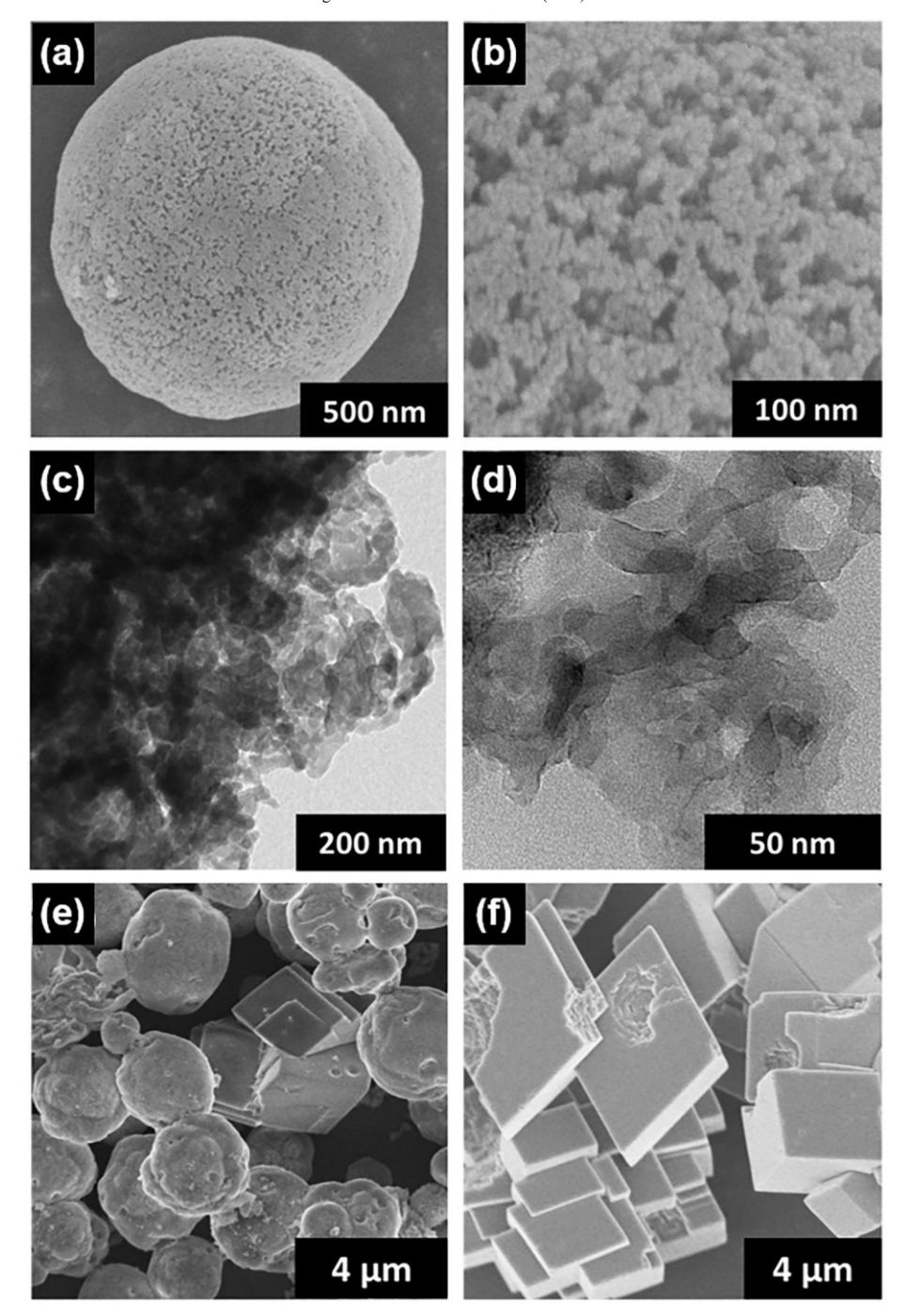
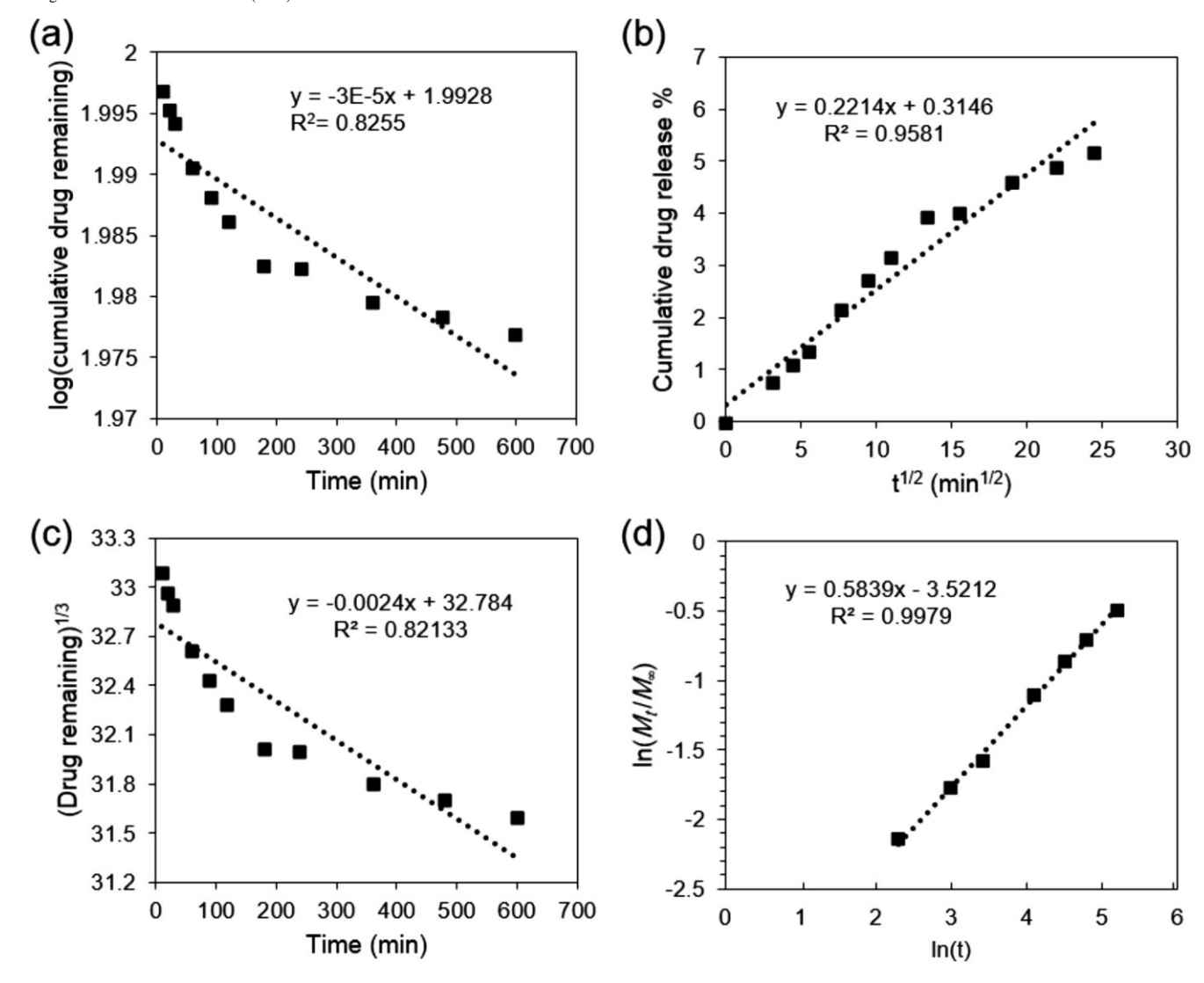


Fig. 2. (a, b) SEM images and (c, d) TEM images of nanoporous CaCO₃ spheres at 25 C. (e, f) SEM images of CaCO₃ synthesized (e) in the presence of PAA-b-PNIPAM at 45 C and (f) in the absence of PAA-b-PNIPAM at 25 C.

145



 $Fig. \ 3. \ Release \ kinetic \ models \ of \ DOX \ from \ nanoporous \ CaCO_3 \ spheres: (a) \ First \ order, (b) \ Higuchi, (c) \ Hixson-Crowell, \ and (d) \ Korsmeyer-Peppas.$

Release kinetic parameters of DOX from nanoporous CaCO₃ spheres.

First order	Higuchi			Hixson-Crowell		Korsmeyer-Peppas		
K ₁ (min ¹)	R ₂	KH (% min1/2)	R2	KHC (min1)	R2	K (min ⁿ)	n	R ₂
0.00003	0.8255	0.2214	0.9581	0.0024	0.8213	0.0295	0.5839	0.9979

plots and are tabulated in Table 1. It is found that the release of DOX from CaCO₃ spheres is in a good agreement with the Higuchi model, which may be attributed to the diffusion of retained DOX through nanoporous CaCO₃ spheres. Furthermore, the high correlation coefficient (R²) value confirms the dependence of the t^{1/2} on the drug release, which is a characteristic factor of Fickian diffusion mechanism [17]. This experimental data fitting with the Higuchi model justifies our approach for monitoring drug release from nanoporous materials under dynamic flow conditions by means of UV-Vis spectroscopy.

As shown in Eq. (5), Peppas used n value to characterize the release mechanisms and concluded that n=0.5 for Fickian diffusion and higher values of exponent n, between 0.5 and 1.0, or n=1.0, for mass transfer following a non-Fickian model of an anomalous release mechanism [17]. From Korsmeyer-Peppas equation, the portion of the release curve $M_t/M_1 < 0.6$ should only be used and an excellent linear fit was obtained, allowing exponent n to be determined from the linear portion of the slope. The calculated value of n is 0.58, indicating that the release mechanism follows a

non-Fickian model of an anomalous release mechanism [17]. The release of DOX would proceed firstly by leaching of free drug molecules from the CaCO₃ pore entrances, thereafter, DOX molecules continue to dissolve slowly into the liquid phase from the CaCO₃ spheres.

4. Conclusion

We synthesized nanoporous CaCO₃ spheres using PAA-bPNIPAM as a structure directing agent. The synthetic method is based on straightforward chemical reactions without the use of complex chemicals. Our approach is widely applicable to synthesize wide range of nanoporous spheres with various properties, by selecting different inorganic precursors. The obtained nanoporous CaCO₃ spheres could be successfully used as a carrier for anticancer drug DOX. Although recently several types of hydroxyapatite particles with different shapes and structures have been applied to biomedical applications because of high biocompatibility [18–21], our CaCO₃ spheres can also be used as a carrier of drugs, proteins, and imaging agent for the development of robust and biocompatible nano-carrier in the future.

Acknowledgement

This work was supported by the Deanship of Scientific Research (DSR), King Abdulaziz University (Grant number KEP-1-130-39), an Australian Research Council (ARC) Future Fellow (Grant number FT150100479), JSPS KAKENHI (Grant numbers 17H05393 and 17K19044), and the research fund by the Suzuken Memorial Foundation.

Appendix A. Supplementary data

Supplementary data associated with this article can be found, in the online version, at https://doi.org/10.1016/j.matlet. 2018.07.060.

S. Guragain et al. / Materials Letters 230 (2018) 143-147

References

- [1] K. Fujihara, M. Kotaki, S. Ramakrishna, Biomaterials 26 (2005) 4139.
- L. Yang, Y. Hu, H. Guo, L. Song, Z. Chen, W. Fan, J. Appl. Pol. Sci. 102 (2006) 2560.
- W. Wei, G.-H. Ma, G. Hu, D. Yu, T. Mcleish, Z.-G. Su, Z.-Y. Shen, J. Am. Chem. Soc. 130 (2008) 15808.
- [4] M.-Q. Gong, J.-L. Wu, B. Chen, R.-X. Zhuo, S.-X. Cheng, Langmuir 31 (2015) 5115.
- [11] B.P. Bastakoti, Y. Li, T. Kimura, Y. Yamauchi, Small 11 (2015) 1992.

- Y. Zhao, Y. Lu, Y. Hu, J.P. Li, L. Dong, L.-N. Lin, S.-H. Yu, Small 6 (2010) 2436.
- D. Zhao, J. Jiang, J. Xu, L. Yang, T. Song, P. Zhang, Mater. Lett. 104 (2013) 28.
- J.L. Arias, M.S. Fernández, Chem. Rev. 108 (2008) 4475.
- L. Qi, J. Li, J. Ma, Adv. Mater. 14 (2002) 300.
- E. Loste, E. Díaz-Martí, A. Zarbakhsh, F.C. Meldrum, Langmuir 19 (2003) 2830.
- [10] T. Nishimura, T. Ito, Y. Yamamoto, M. Yoshio, T. Kato, Angew. Chem. Int. Ed. 47 (2008) 2800
- [12] Y. Li, B.P. Bastakoti, Y. Yamauchi, APL Mater. 4 (2016) 040703.
- [13] S. Guragain, B.P. Bastakoti, V. Malgras, K. Nakashima, Y. Yamauchi, Chem. Eur. J. 21 (2015) 13164.
- [14] T. Tomida, K. Hamaguchi, S. Tunashima, M. Katoh, S. Masuda, Ind. Eng. Chem. Res. 40 (2001) 3557.
- [15] S. Guragain, B.P. Bastakoti, K. Nakashima, J. Colloid Interface Sci. 350 (2010) 63.
- [16] M.M. Ayad, N.A. Salahuddin, N.L. Torad, A. Abu El-Nasr, RSC Adv. 6 (2016) 57929.
- [17] P. Costa, J.M.S. Lobo, Eur. J. Pharm. Sci. 13 (2001) 123.
- [18] Y.H. Yang, C.H. Liu, Y.H. Liang, F.H. Lin, K.C.W. Wu, J. Mater. Chem. B 1 (2013) 2447.
- [19] B.P. Bastakoti, Y.C. Hsu, S.H. Liao, K.C.W. Wu, M. Inoue, S. Yusa, K. Nakashima, Y. Yamauchi, Chem. Asian J. 8 (2013) 1301.

147

- [20] B.P. Bastakoti, M. Inoue, S. Yusa, S.H. Liao, K.C.W. Wu, K. Nakashima, Y. Yamauchi, Chem. Commun. 48 (2012) 6532.
- [21] Y.H. Liang, C.H. Liu, S.H. Liao, Y.Y. Lin, H.W. Tang, S.Y. Liu, I.R. Lai, K.C.W. Wu, ACS Appl. Mater. Interfaces 4 (2012) 6720.